



Two-Stage Fault Detection and Control Approach for DFIG-Based Wind Energy Conversion System

Daison Stallon¹^a, Ichrak Eben Zaid²^b and Yolanda Vidal^{1,3}^c

¹Control, Data, and Artificial Intelligence (CoDALab), Department of Mathematics, Escola d'Enginyeria de Barcelona Est (EEBE), Universitat Politècnica de Catalunya (UPC), Barcelona, Spain

²Commande Numérique des Procédés Industriels (CONPRI) National School of Engineers of Gabes, University of Gabes, Tunisia

³Institut de Matemàtiques de la UPC, BarcelonaTech, IMTech, Pau Gargallo 14, 08028 Barcelona, Spain

Keywords: Wind Turbines, Wind Speed, Fault Diagnosis, Wind Energy Conversion Systems, Control Monitoring, Doubly Fed Induction Generators, Machine Learning.

Abstract: Doubly-Fed Induction Generator (DFIG)-based Wind Energy Conversion Systems (WECS) are critical in modern electricity generation due to their ability to enhance energy capture and seamlessly integrate with the electrical grid. However, maintaining reliability and minimizing maintenance costs are essential to ensure consistent energy production. This research presents an innovative method for fault detection and diagnosis in DFIG-based WECS. The approach leverages independent component analysis-based correlation coefficient for precise fault identification. Additionally, an enhanced multihead cross attention with bi-directional long short term memory classifier is employed to accurately categorize different fault types. To further improve classifier's performance, the multi-strategy enhanced orchard algorithm is implemented, focusing on regulating active and reactive power variations, harmonics in rotor current, and voltage in the DC link. The proposed method is evaluated using MATLAB working platform and demonstrates a high accuracy rate of 98% compared to other techniques.


1 INTRODUCTION


The increasing use of fossil fuels and growing environmental concerns highlight the urgent need for clean and sustainable energy sources. Wind energy has become a vital part of the global energy landscape, providing 20% of the world's electricity, with Wind Turbines (WT) at its core. Consequently, efficient problem diagnosis and maintenance are necessary to ensure that WT operates dependably (Ding et al., 2019; Heilari et al., 2016). Power electronic converters' fault-tolerant performance in a variety of applications, including electrical drives, has been extensively studied in recent years. Zhang et al. (2014), for instance, talk about fault-tolerant techniques for multilevel and two-level converters. Furthermore, Riera-Guasp et al. (2014) offer information on condition monitoring and fault-


tolerant operation for electric drives and other equipment.

Moreover, a fault-tolerant control strategy for a T-type three-level inverter is presented which guarantees a decrease in power and output voltage distortions in the event of an open circuit fault. Despite the paucity of research on fault tolerance in Wind Energy Conversion Systems (WECSs), provides a fault-tolerant topology using a five-leg converter configuration for the grid side converter's post-fault operation in PMSG-based systems. An alternative approach is presented, wherein the output phases are connected to the dc-link post-fault detection midway.

Practicality is limited, though, as this arrangement causes grid-side converter switch voltages to double in the post-fault mode (Li, Y et al. 2020; Tumari, M et al. 2022; Dou, B et al. 2020). To eliminate current

^a <https://orcid.org/0000-0002-1339-6919>

^b <https://orcid.org/0000-0001-5066-3601>

^c <https://orcid.org/0000-0003-4964-6948>

distortion post-fault, research suggests fault-tolerant control for open-switch faults in three-level neutral point clamped converters of Permanent Magnet Synchronous Generator (PMSG) based systems by using d-axis current injection. References (SaeKok et al., 2010), examined the reconfiguration post-fault diagnosis and converter defects in DFIG. Kanjiya et al. (2013) presented a fault-tolerant Power Electronic (PE) structure by substituting a nine-switch Grid Side Converter (GSC).

While grid failures are covered in (Li et al., 2014), converter faults are not mentioned. Shi and Patton (2015) explain current sensor malfunctions and introduce a new current observer to enhance fault detection. In order to overcome these problems, Gao et al. (2015a) investigate malfunctions in pitch and generator speed sensors and suggest an observer-based active fault-tolerant control technique.

Timely defect detection is critical to all fault-tolerant

systems. A wealth of information on defect diagnostic techniques has been published recently, including surveys such as (Gao et al., 2015b).

Various research papers have existed in the literature

based on fault analysis in wind energy using various techniques and aspects. Tuerxun et al. (Tuerxun et al., 2021) introduced the SSA-SVM (Sparrow Search Algorithm-Support Vector Machines) model, an efficient approach that outperforms existing methods for enhancing diagnostic accuracy and applicability of WT. Zhang et al. (Zhang et al., 2022) introduced a CVAE-GAN (Conditional Variational Generative Adversarial Network)-based strategy, enhancing the diagnostic precision of WT in complex scenarios.

Kong et al. (Kong et al., 2021) introduced an adaptive noise reduction technique known as CDWPSO (Chaotic Dynamic Weight Particle Swarm Optimization with Sigmoid-Based Acceleration Coefficients), aimed at enhancing the diagnosis of bearing faults in WT.

Hsu et al. (Hsu et al., 2020) employed a statistical process control and machine learning on 2.8 million sensor data to diagnose WT faults and predict maintenance needs with high accuracy, improving operational efficiency and reducing downtime. Qi et al. (Qi et al., 2023) presented the WJDAN (Weighted Joint Domain Adversarial Network) as an innovative approach for improving cross-domain fault diagnosis in WT. This research makes the following significant contributions:

- To handle the non-stationary nature of vibration signals originating from WECS, the research

uses the Independent Component Analysis-based Correlation Coefficient (ICA-CC) method, particularly within the timefrequency domains.

- The research encompasses the process of training an Enhanced Multihead Cross Attention with BiLSTM (EMCABN) classifier, that is specifically designed for categorizing different types of faults in WECS.
- Furthermore, the research involves the optimization of critical parameters within the EMCABN model.
- This optimization is carried out using the Multi-strategy Enhanced Orchard Algorithm (MSEOA) for controlling the variations in active and reactive powers, harmonics in rotor current, and the voltage in the dc-link.

The research is organized into distinct sections: Section 2 outlines the proposed control methodology mechanism, Section 3 discusses implementation results, and Section 4 offers a comprehensive conclusion summarizing the entire work.

2 PROPOSED SYSTEM UNDER INVESTIGATION

The data processing system depicted in Figure 1 for WT fault detection and classification represents a cutting-edge and comprehensive approach to ensuring the reliability and safety of WT while also mitigating maintenance costs. The present framework comprises the following primary steps for the goal of defect identification and classification:

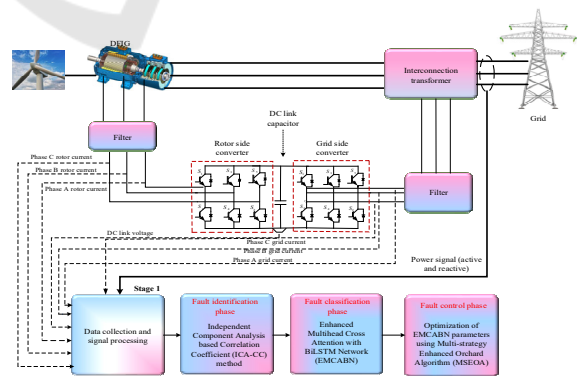


Figure 1: Structure of proposed methodology.

Data Collection: Under various operating conditions, the process records different measurements. The gathered data depicts both optimal and several potentially flawed scenarios that

may arise during the process. It can be split into two sets, one for testing and the other for training.

Denoising Process: Firstly, use the wavelet threshold denoising method to denoise the defected voltage signal, then the denoised voltage signal is subjected to ICA-CC model to produce a series of components.

Feature Extraction: When the system is functioning normally, an ICA-CC model is constructed solely from the training data set. The ICA-CC model extracts a collection of characteristics where the original data's information becomes less and less important. As a result, the features that are most frequently caught are retained and show how the data is projected onto a subspace that is determined by fewer total projector directions. Given that it has a substantial impact on the classification performance, this quantity was chosen with sufficient care. The combined probabilities of the chosen features across the various process scenarios are computed. An ICA-CC model with five directions has been built based on the most important information that was projected from the data.

Fault Detection and Classification: During the training phase, EMCABN demonstrates a potential capacity to identify each of the WT's various operating circumstances. The quantity of situations determines the EMCABN structure. As a result, each scenario is given a matching state. The intermediate transitions between all EMCABN states are defined manually based on certain requirements and for large-sized data. Conversely, estimating the transition probabilities is more feasible in the univariate scenario. The EMCABN parameter triplet is defined once it has been trained, and its effectiveness is evaluated using a testing setup.

Fault Control: Wind speed, rotor speed, generator temperature, voltage, and current are the inputs of the system. Using these inputs, fault control actions are implemented, such as adjusting pitch angle, yaw control, braking, or activating protection mechanisms to mitigate fault effects and ensure safe and efficient WECS operation. The mechanism is done using MSEOA.

2.1 Fault Identification Phase Using ICA-CC

In the fault detection phase of the DFIG-based WECS, the independent component analysis-based correlation coefficient (ICA-CC) is used to isolate and identify fault signatures from the system's operational data. The ICA-CC method effectively separates the mixed signals into independent components, allowing for precise detection of

anomalies indicative of faults.

Monitoring statistics include active and reactive power variations, harmonics in rotor currents, and voltage fluctuations in the DC link. These parameters are continuously monitored to establish baselines and identify deviations that may signal a fault. Thresholds for each parameter are set based on historical data, and any significant deviation triggers an alert. The enhanced multihead cross attention with BiLSTM classifier then categorizes the fault type based on the identified patterns, ensuring accurate and timely diagnosis. The monitoring statistics are crucial in this phase, as they provide the necessary data to detect and classify faults efficiently.

Fault Detection:

Input Parameters: Decrease in wind speed, abnormal generator temperature rise, and fluctuations in electrical grid voltage.

Output: Detection of anomalies in the system's behavior, triggering an alarm for further investigation.

Based on this, the measured data matrix is represented in the following:

$$X = AS + E \quad (1)$$

Where X represents the measured data matrix, S represents the independent component matrix, and A represents the mixing matrix. To find the separation matrix W , the reconstructed matrix \hat{S} is derived as follows:

$$\hat{S} = WX \quad (2)$$

To derive the detection logic, the thresholds are established first, followed by the application of the corresponding logic:

$$\begin{cases} I^2 < J_{I_{th}^2} & \& \text{SPE} < J_{SPE,th} \Rightarrow \text{fault - free} \\ I^2 \geq J_{I_{th}^2} & \& \text{SPE} \geq J_{SPE,th} \Rightarrow \text{fault - occurred} \end{cases} \quad (3)$$

where estimated thresholds are expressed as J_2 and $J_{SPE,th}$, the unit matrix is expressed as I .

2.2 Fault Classification Phase Using EMCABN

The fault classification phase in DFIG-based WECS leverages the Enhanced Multihead Cross Attention with BiLSTM Network (EMCABN) to accurately categorize various fault types (Leng, X.L et al. 2021). This advanced model combines the strengths of multihead attention mechanisms and BiLSTM

networks. The model can focus on various input data points at once thanks to the multihead cross attention method, which helps it identify complex patterns linked to various defects. The BiLSTM component, with its bidirectional processing, ensures that temporal dependencies in the data are effectively utilized, leading to a more accurate fault classification.

EMCABN excels in handling complex, nonlinear relationships within the system, enabling it to differentiate between subtle fault signatures. By integrating this approach, the model can classify faults with high precision, which is essential for timely intervention and maintenance in WECS. The performance of EMCABN is further enhanced by optimizing its parameters using the Multi-strategy Enhanced Orchard Algorithm (MSEOA), ensuring robust classification under various operational conditions.

Fault Classification:

Input Parameters: Detected anomalies and historical fault data.

Output: Classification of faults into categories such as mechanical faults (e.g., bearing failure), electrical faults (e.g., short-circuit in the generator), or gridrelated faults (e.g., voltage instability).

It incorporates the forward hidden layer denoted as L_{fw} , the backward hidden layer L_{bw} and the output GHI_{Op} for network updates. The network undergoes iterative updates, proceeding both in the backward direction, beginning T to 1 and in the forward direction, beginning 1 to T . The mathematical expression for the layers of the EMCABN technique is formulated as follows:

$$L_{fw} = \sigma(w_1 GHI_i(t) + w_2 L_{f-1} + b_{L_f}) \quad (4)$$

$$L_{bw} = \sigma(w_3 GHI_i(t) + w_5 L_{b-1} + b_{L_b}) \quad (5)$$

$$GHI_{Op} = w_4 L_f + w_6 L + b_{GHI_O} \quad (6)$$

where, L_{fw} represents forward bias, L_{bw} represents backward pass, GHI_{Op} represents the final output layers. σ represents standard deviation, w represents the weight coefficients, and b_{L_f} , b_{L_b} , and b_{GHI_O} defines the biases in the model.

2.3 Fault Control Phase Using MSEOA

The practical implementation of a multi-objective framework for WT fault detection is discussed in this section. This framework's main goal is to maximise EMCABN. The objective function for the proposed system is formulated in the following.

Objective function = min (E)

$$E = [V_{DC}, I_{r,abc}, V_{r,abc}, I_{g,abc}, V_{g,abc}, P, Q] \quad (7)$$

where, error is specified as E which mainly defines the minimization of voltage, current and power variation in the WECS. V_{DC} represents dc-link voltage, $I_{r,abc}$, $V_{r,abc}$ represents three phase rotor current and voltage, $I_{g,abc}$, $V_{g,abc}$ represents three phase grid current and voltage, P represents active power, Q represents reactive power, 'min' represents minimize.

Fault Control:

Input Parameters: Identified fault types and system configuration.

Output: Implementation of control actions such as adjusting pitch angle to reduce load on the turbine or activating protection mechanisms to isolate faulty components. Pseudocode and flowchart of MSEOA is shown in Figure 2 respectively.

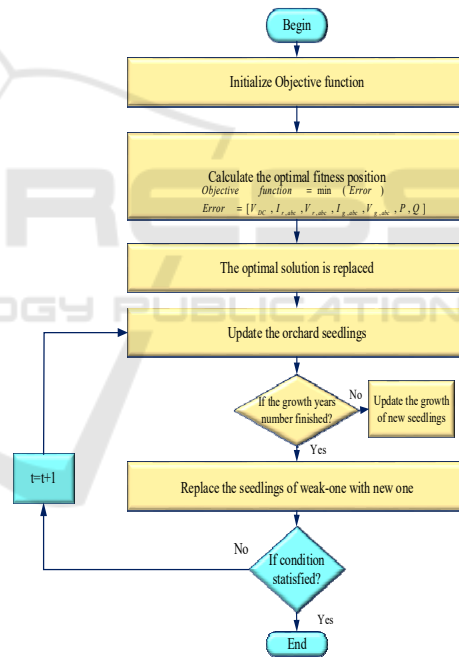


Figure 2: Flowchart of MSEOA Algorithm.

2.4 Step-by-Step Explanation of Multi-Strategy Enhanced Orchard Algorithm (MSEOA)

According to the Orchard Algorithm (OA), exploration is the movement of candidate individuals in the direction of the ocean current, whereas exploitation is the movement of candidate individuals within the swarm. Temporal control

parameters regulate how these two phases transition into one another. In Kaveh et al., 2023.

In order to find potential areas, the OA focusses on exploration in the beginning of an iteration. Ultimately, though, the OA favors exploitation to identify the optimal spot inside the designated region.

The algorithm's capacity for local exploration and convergence are enhanced by the sine and cosine learning factors approach. The ability to participate in global exploitation and to break free from the trap of local optimization is both improved by the local escape operator method. Opposition Based Learning (OBL) and Quasi Oppositional Learning (QOL) approaches increase the population solution quality and expand the pool of possible persons, which improves optimization competency. An MSEOA is created by integrating the OA with these three tactics. In order to solve optimisation difficulties, MSEOA integrates multiple sophisticated methodologies, building upon the fundamentals of OA. To improve the OA, it combines generalised oppositional learning, quadratic interpolation, and orthogonal learning. Generalised oppositional learning enhances initial population quality and convergence, quadratic interpolation improves the accuracy of global searches, and orthogonal learning helps escape local optima. When combined, these tactics improve OA performance, especially for high-dimensional and complicated issues. The comprehensive steps of the MSEOA are summed up in the following to represent the aforementioned phases.

Step 1. Start by initializing a population of solutions randomly. Each solution represents a potential answer to the optimization problem, and the population size determines the number of solutions considered at each iteration. Define necessary parameters, such as the number of iterations, the search space boundaries, and the learning rates. Initialize specific parameters for each strategy used within the algorithm. Establish $N = 300$ and $T = 200$, specify the fitness function, and use the logistic maps provided by to create the starting locations of N seedlings in the solution search space. $P_{i+1} = \alpha P_i(1 - P_i)$, $0 \leq P_0 \leq 1$ and let $t = 1$.

Step 2. Assess and contrast the objective value of every contender, and record the best location thus far along with the matching optimal objective value. Evaluate the fitness of each solution using an objective function. This function quantifies how well each solution solves the problem. In DFIG-based WECS, for instance, it could measure how well the algorithm controls power variations and harmonics.

Rank the solutions based on their fitness. The better the solution, the higher its rank.

Step 3. Growth of the seedlings. Compute the time control function $C(t)$. If $C(t) > 0.5$, the candidate individual $P_i(t)$ tracts the growth for each seedling, screening of the seedlings and graft for each seedling $P_i(t+1)$ is renewed using

$$P_i(t+1) = P_i(t) + r2 \times (P^* - \beta \times r2 \times \mu).$$

Where constants is denoted as β , μ , random number is expressed as $r2$, deviated updated position is denoted as P^* .

Step 4. Replacement of the weak seedlings by the new ones. If $rand(0,1) > (1 - C(t))$, Type A movement is performed by the candidate, and the new position is determined using $P_i(t+1) = P_i(t) + \gamma \times r3 \times (Ub - Lb)$.

Otherwise, the candidate engaged in Type B movement, and the updated position makes use of

$$P_i(t+1) = \omega_1 \cdot (P_i(t) + \overrightarrow{step}) + \omega_2 \cdot (P^* - P_i(t)).$$

Where, upper bound and lower bound is expressed as Ub, Lb , constant for seedlings is expressed as γ , \overrightarrow{step} is expressed as step function.

Step 5. Verify the modified individual solution to see if it exceeds the boundary condition. If it is outside the scope of the search, $\bar{P}_i^d = rand\left(\frac{Lb^d + Ub^d}{2}, Lb^d + Ub^d - P_i^d\right)$ is used to return to the opposite boundary.

Step 6. Examine the current location's objective cost both before and after upgrading. Replace the site if the grafted seedlings are more fit than the existing one. Next, compare the ideal fitness value to the objective value of the existing place. Renew the best location so far found and the accompanying ideal objective value if the objective value at the current position is superior.

Step 7. If $t < T$, go back to Step 3, otherwise, perform Step 8.

Step 8. The optimal solution is the one that remains after the algorithm converges and finds the best solution. Next, this solution is implemented in the problem domain, e.g., DFIG-based WECS fault categorisation. In order to confirm the solution's

resilience, evaluate the outcomes once more and, if necessary, validate the results against different benchmarks.

3 RESULTS AND DISCUSSION

The research uses a benchmark model that uses the MATLAB software to simulate a modern WT in order to evaluate the efficacy of this strategy (Xiahou, K.S et al 2020). The dataset consisting of images related to these fault scenarios, is divided into two subsets through a random split. Details on the number of variables assessed, the total number of samples, and the percentage of data allotted to training and testing should all be included in the EMCABN dataset.

Usually, 80% of the data is used for training and 20% is used for testing; however, this could change depending on the study. The Multihead Cross Attention mechanism improves the model's focus on pertinent portions of the input data, enhancing overall performance in tasks like time series prediction or classification. The EMCABN catches both past and future information in the sequence. Simulink block setup of the proposed system is shown in Figure 3.

Approximately 75% of these images are allocated for detection within the EMCABN, while the remaining 25% are reserved for the classification task.

Figure 4 shows the average accuracy of the EMCABN-MSEOA machine learning model over the course of training. The validation accuracy reaches a maximum of about 98% at around epoch 10. The proposed EMCABN detects the WT faults with remarkable average accuracy of 98%. The Figure 5 shows the training and validation loss of a machine learning model over the course of training. The results, shown in Figure 6, indicate that EMCABN-MSEOA benefit from increased depth. Notably, EMCABN-MSEOA models with two or three layers achieved performance, reaching an F1 score of about 98%. This represents a substantial 7% improvement over the single-layer EMCABNMSEOA model.

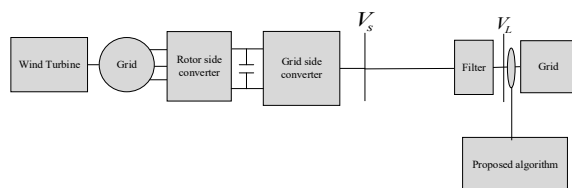


Figure 3: Simulink block setup of the proposed system.

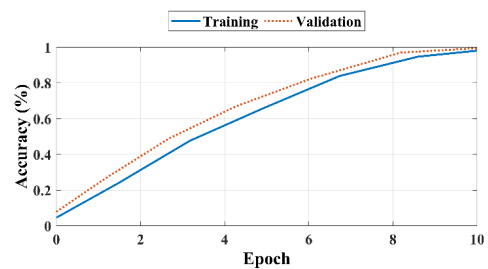


Figure 4: Average accuracy of the EMCABN-MSEOA model.

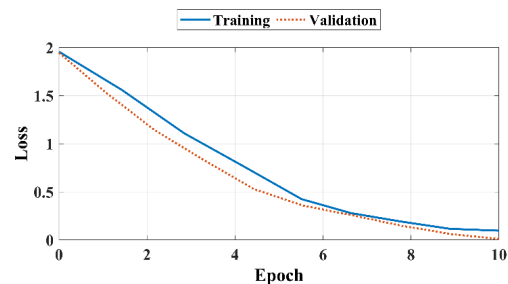


Figure 5: Average losses of the EMCABN-MSEOA model.

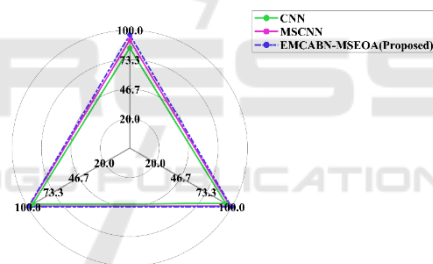


Figure 6: Comparison for efficient diagnosis of WT fault with proposed and conventional techniques.

In Figure 7, the evaluation compares EMCABNMSEOA, MSCNN, and CNN using average F1 scores across eight conditions as the evaluation metric. Table 1 offers a comprehensive and wellrounded analysis by synthesizing the results from 50 randomly conducted trials.

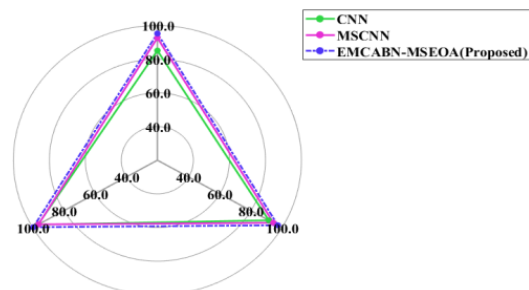


Figure 7: Comparison for efficient diagnosis of noise with proposed and conventional techniques.

Table 1: Comparison of solution techniques for 50 random trails.

Techniques	F_1 Score (%)	Detection time (s)
CNN (Zare and Ayati, 2021)	98.82±0.0050	36.7318±0.2197
MSCNN (Zare and Ayati, 2021)	98.57±0.0038	14.5388±0.2247
EMCABN-MSEOA	98.05±0.0058	14.5995±0.1756
Techniques	Classification time (ms)	Control time(s)
CNN (Zare and Ayati, 2021)	0.4884±0.0023	6.56
MSCNN (Zare and Ayati, 2021)	0.1806±0.0025	4.19
EMCABN-MSEOA	0.1814±0.0022	2.65

Table 2: Comparison of solution techniques for 50 random trails.

Techniques	Control level 1	Control level 2	Control level 3
CNN (Zare and Ayati, 2021)	80.41±4.32	86.92±2.84	72.50±5.40
MSCNN (Zare and Ayati, 2021)	71.01±1.04	70.42±2.32	62.70±3.04
EMCABN-MSEOA	97.34±0.96	98.20±0.72	96.76±1.46
Techniques	Control level 4	Control level 5	Average
CNN (Zare and Ayati, 2021)	96.93±2.99	78.95±3.21	84.31
MSCNN (Zare and Ayati, 2021)	72.09±1.97	71.30±1.57	72.71
EMCABN-MSEOA	98.94±0.85	99.05±0.69	98.33

Within Table 2, a comprehensive comparative assessment is presented, utilizing percentage scores as the evaluative metric. Statistical comparative analysis is shown in Table 3. The performance of proposed technique is compared with existing approaches (Dhibi, K et al. 2022) such as NN-based EL (NN-EL), Reduced NN-EL, Neural Network (NN), Bagging ensemble, Random Forest ensemble, Cascade Forward Neural Network (CFNN), Multiple Layers (MNN), Feed-Forward Neural Network (FFNN), and Generalized Regression Neural Network (GRNN).

The proposed method gives better results in terms of statistical analysis.

Table 3: Statistical comparative analysis.

Methods	Global performances			
	Accuracy	Recall	Precision	Computational time (s)
Proposed	99.98	99.987	99.987	27.01
GRNN	97.01	97.01	97.01	99.14
FFNN	97.17	97.18	97.17	126.45
MNN	93.58	93.58	93.58	51.30
CFNN	97.41	97.41	97.40	186.82
Random Forest ensemble	98.41	98.41	98.42	261.3
Bagging ensemble	98.31	98.31	98.31	197.12
NN	93.70	93.71	93.70	47.01
Reduced NN-EL	99.95	99.95	99.95	141
NN-EL	99.97	99.97	99.97	386

Table 4 displays the results of the Wilcoxon signed-rank test comparison (Fathy, A. et al., 2022). The suggested approach differs dramatically, with a 95% confidence level.

Table 4: Wilcoxon signed-rank test comparison results.

Method	Negative ranks	Positive ranks	Ties	Z	Decision regard (30 runs)
GA-PSO	5 ^a	25 ^b	0 ^c	-3.918 ^d	a. GA < PSO b. GA > PSO c. GA = PSO d. Based on negative ranks
FPA-GA	30 ^a	0 ^b	0 ^c	-4.782 ^d	a. FPA < GA b. FPA > GA c. FPA = GA d. Based on positive ranks
FPA-PSO	30 ^a	0 ^b	0 ^c	-4.782 ^d	a. FPA < PSO b. FPA > PSO c. FPA = PSO d. Based on positive ranks
Proposed	35 ^a	0 ^b	0 ^c	-5 ^d	a. Proposed < FPA-GA b. Proposed > FPA-GA c. Proposed = FPA-GA d. Based on positive ranks

4 CONCLUSIONS

This work confirms the efficacy of the EMCABNMSEOA method in processing signal images for intelligent WT fault diagnosis, which improves system reliability and reduces the need for human interpretation. The methodology is shown to be proficient at detecting faults and accelerating the decision-making process, thereby decreasing the dependence on human expertise for signal feature extraction. Variable wind speeds, a significant factor influencing WT performance, are incorporated into the analysis. Utilizing data across various wind speeds ensures that the approach reflects real-life scenarios. When compared to other artificial neural networks, the Independent Component Analysis-based Correlation Coefficient (ICA-CC) is notable for its ability to directly extract optimal features from raw data, although it does necessitate a considerable amount of training data. Additionally, the EMCABN-MSEOA method is characterized by its computational efficiency and an impressive classification accuracy rate of 98%, representing a notable improvement. Future works are planned to apply this method to actual vibration data from WT gearboxes in wind farms to confirm its practical value in improving operational WT fault diagnosis.

ACKNOWLEDGEMENTS

This work was supported by the Spanish Agencia

Estatal de Investigació'n (AEI) Ministerio de Economía, Industria y Competitividad (MINECO), and the Fondo Europeo de Desarrollo Regional (FEDER) through the research projects PID2021122132OB-C21 and TED2021-129512B-I00; and by the Generalitat de Catalunya through the research project 2021-SGR-01044.

REFERENCES

- Dou, B., Qu, T., Lei, L. and Zeng, P., (2020). Optimization of wind turbine yaw angles in a wind farm using a three-dimensional yawed wake model. *Energy*, 209, p.118415.
- Ding, P., Wang, H., Bao, W., and Hong, R. (2019). Hygmsam based model for slewing bearing residual useful life prediction. *Measurement*, 141:162–175.
- Dhibi, K., Mansouri, M., Bouzrara, K., Nounou, H. and Nounou, M., (2022). Reduced neural network based ensemble approach for fault detection and diagnosis of wind energy converter systems. *Renewable Energy*, 194, pp.778-787.
- Fathy, A., Rezk, H., Yousri, D., Kandil, T. and Abo-Khalil, A.G., (2022). Real-time bald eagle search approach for tracking the maximum generated power of wind energy conversion system. *Energy*, 249, p.123661.
- Gao, Z., Cecati, C., and Ding, S. X. (2015a). A survey of fault diagnosis and fault-tolerant techniques—part i: Fault diagnosis with model-based and signal-based approaches. *IEEE transactions on industrial electronics*, 62(6):3757–3767.
- Gao, Z., Cecati, C., and Ding, S. X. (2015b). A survey of fault diagnosis and fault-tolerant techniques—part i: Fault diagnosis with model-based and signal-based approaches. *IEEE transactions on industrial electronics*, 62(6):3757–3767.
- Heidari, M., Homaei, H., Golestanian, H., and Heidari, A. (2016). Fault diagnosis of gearboxes using wavelet support vector machine, least square support vector machine and wavelet packet transform. *Journal of Vibroengineering*, 18(2):860–875
- Hsu, J.-Y., Wang, Y.-F., Lin, K.-C., Chen, M.-Y., and Hsu, J. H.-Y. (2020). Wind turbine fault diagnosis and predictive maintenance through statistical process control and machine learning. *Ieee Access*, 8:23427–23439.
- Kanjiya, P., Ambati, B. B., and Khadkikar, V. (2013). A novel fault-tolerant dfig-based wind energy conversion system for seamless operation during grid faults. *IEEE Transactions on Power Systems*, 29(3):1296–1305.
- Kaveh, M., Mesgari, M.S. and Saeidian, B., (2023). Orchard Algorithm (OA): A new meta-heuristic algorithm for solving discrete and continuous optimization problems. *Mathematics and Computers in Simulation*, 208, pp.95-135.
- Kong, X., Xu, T., Ji, J., Zou, F., Yuan, W., and Zhang, L. (2021). Wind turbine bearing incipient fault diagnosis based on adaptive exponential wavelet threshold function with improved cpso. *Ieee Access*, 9:122457–122473.
- Leng, X.L., Miao, X.A. and Liu, T., (2021). Using recurrent neural network structure with enhanced multi-head self-attention for sentiment analysis. *Multimedia Tools and Applications*, 80, pp.12581-12600.
- Li, Y., Wei, K., Yang, W. and Wang, Q., (2020). Improving wind turbine blade based on multi-objective particle swarm optimization. *Renewable Energy*, 161, pp.525-542
- Li, H., Yang, C., Hu, Y., Zhao, B., Zhao, M., and Chen, Z. (2014). Fault-tolerant control for current sensors of doubly fed induction generators based on an improved fault detection method. *Measurement*, 47:929–937.
- Qi, H., Han, Y., Tuo, S., and Zhao, Q. (2023). Fault diagnosis in wind turbines based on weighted joint domain adversarial network under various working conditions. *IEEE Sensors Journal*.
- Riera-Guasp, M., Antonino-Daviu, J. A., and Capolino, G. A. (2014). Advances in electrical machine, power electronic, and drive condition monitoring and fault detection: State of the art. *IEEE Transactions on Industrial Electronics*, 62(3):1746–1759.
- Sae-Kok, W., Grant, D., and Williams, B. (2010). System reconfiguration under open-switch faults in a doubly fed induction machine. *IET Renewable Power Generation*, 4(5):458–470.
- Shi, F. and Patton, R. (2015). An active fault tolerant control approach to an offshore wind turbine model. *Renewable Energy*, 75:788–798.
- Tuerxun, W., Chang, X., Hongyu, G., Zhijie, J., and Huajian, Z. (2021). Fault diagnosis of wind turbines based on a support vector machine optimized by the sparrow search algorithm. *Ieee Access*, 9:69307–69315.
- Tumari, M.Z.M., Ahmad, M.A., Suid, M.H. and Ghazali, M.R., (2022), December. Data-driven control based on marine predators algorithm for optimal tuning of the wind plant. In 2022 IEEE International Conference on Power and Energy (PECon) (pp. 203-208). IEEE.
- Xiahou, K.S., Liu, Y., Li, M.S. and Wu, Q.H., (2020). Sensor fault-tolerant control of DFIG based wind energy conversion systems. *International Journal of Electrical Power & Energy Systems*, 117, p.105563.
- Zare, S. and Ayati, M. (2021). Simultaneous fault diagnosis of wind turbine using multichannel convolutional neural networks. *ISA transactions*, 108:230–239.
- Zhang, L., Zhang, H., and Cai, G. (2022). The multiclass fault diagnosis of wind turbine bearing based on multisource signal fusion and deep learning generative model. *IEEE Transactions on Instrumentation and Measurement*, 71:1–12.
- Zhang, W., Xu, D., Enjeti, P. N., Li, H., Hawke, J. T., and Krishnamoorthy, H. S. (2014). Survey on fault-tolerant techniques for power electronic converters. *IEEE Transactions on Power Electronics*, 29(12):6319–6331.